Journal of Aerosol Science 101 (2016) 34–42

Contents lists available at ScienceDirect

Journal of Aerosol Science

journal homepage: www.elsevier.com/locate/jaerosci

Technical note

Parametric investigation of two aerosol scavenging models in the inertial regime

S. Fredericks, J.R. Saylor *

Department of Mechanical Engineering, Clemson University, Clemson, SC 29634-0921, United States

ARTICLE INFO

Article history:
Received 22 March 2016
Received in revised form
30 June 2016
Accepted 13 July 2016
Available online 20 July 2016

Keywords:
Scavenging
Particles
Drops
Inertial impaction

ABSTRACT

Models of drop scavenging of aerosols via inertial impaction proposed by Slinn and by Calvert are compared with published experimental measurements to determine which model is a better predictor of the data. Additionally, a parametric study was performed on the residual of the model predictions from the measurements to identify dimensionless groups not included in these models, which might increase model performance. The study found that the Calvert model predicts scavenging in the inertial regime with less error than the Slinn model. The study also found that two dimensionless groups, the relative Stokes number, Stk_r, and the drop Reynolds number, Re_D, are both well correlated with the residual of these models. They are included in modified versions of both of these models to provide better performance. That these two dimensionless groups improve model performance suggests that an inertial mechanism and an advective mechanism not accounted for in the existing models play some role in aerosol scavenging in the inertial regime.

1. Introduction

Understanding how a drop, such as a rain drop or a spray drop, removes aerosols has a wide range of applications, from atmospheric particulate removal (Greenfield, 1957) and climate modeling (Adams & Seinfeld, 2002; Roeckner et al., 2003; Wang, Zhang, & Moran, 2010; Webster & Thomson, 2014) to dust control in mining and industrial processes (Calvert & Goldshmid, 1972; Kissell, 2003; Schnelle & Brown, 2002; Walton & Woolcock, 1960). Aerosol scavenging by drops is quantified by the scavenging coefficient, E, which is the ratio of the number of particles collected by the drop, n_c, to the total number of particles within the air column through which the drop passed, n_t:

$$E = \frac{n_c}{n_t} \tag{1}$$

which ranges from zero to unity. The streamlines around a drop do not intersect that drop, and so values for E are primarily caused by particles deviating from the streamline that they are on (an exception to this statement being the interception mode of scavenging, described below). For example, a relatively large particle will have significant inertia and will deviate from its streamline as that streamline curves around the drop, impacting the drop, and causing the particle to be scavenged from the flow. This is called the inertial mode of deposition (Beard & Grover, 1974; Hinds, 1982; Langmuir, 1948; Slinn, 1984),

* Corresponding author.
E-mail address: jsaylor@clemson.edu (J.R. Saylor).

http://dx.doi.org/10.1016/j.jaerosci.2016.07.011
0021-8502/

and is the scavenging mode which this paper is focused upon. In contrast, for particles that are very small and have essentially zero inertia, Brownian motion can cause the particles to deviate from their streamlines, moving toward the drop. This is referred to as diffusional deposition (Hinds, 1982; Levich, 1962; Slinn, 1984). Finally, particles that nominally remain on their streamline, but are on a streamline that comes within half the particle diameter from the drop surface will strike the drop, a process called interception (Friedlander, 1977; Hinds, 1982; Slinn, 1984). In addition to these three primary modes of deposition, there also exist particle scavenging due to processes such as phoretic effects and charging (Park, Jung, Jung, Lee, & Wet, 2005; Slinn, 1984; Wang et al., 2010). The reader is referred to Wang, Leong, Stukel, and Hopke (1983) for a more detailed discussion of these various mechanisms.

One goal of the present work is to determine whether the inertial model due to Slinn (1984) and Slinn et al. (1977) or the inertial model due to Calvert and Englund (1984) and Calvert (1970) (described in detail below) is more accurate by comparing their predictions to experimentally measured scavenging coefficients, E_m. The second goal of this work is to identify additional dimensionless groups that can be used to improve these models so that they better predict E_m. In addition to providing improved versions of the two models, it is hoped that the identified dimensionless groups will help to identify other physical mechanisms which play a role in the inertially dominant scavenging regime.

2. Model descriptions

The present study is focused on models for the inertial mechanism of scavenging. There are only two models used for inertial impaction in the recent literature surveyed (Ardon-Dryer, Huang, & Cziczo, 2015; Chate, Murugavel, Tiwari, & Beig, 2011; Davenport & Peters, 1978; Park et al., 2005; Seinfeld & Pandis, 2006; Wang et al., 2010): the model due to Slinn (1984) and Slinn et al. (1977) and the model due to Calvert and Englund (1984) and Calvert (1970). Both of these models are empirical fits: the Slinn model for scavenging via inertial impaction is a fit to numerical simulations due to Beard and Grover (1974), and the Calvert model for scavenging via inertial impaction is a fit to the experimental results of Walton and Woolcock (1960). Both models are predictions of the contribution of inertial impaction to the scavenging coefficient E and will be referred to hereinafter as E_S and E_C for Slinn and Calvert, respectively. Also, the thing being scavenged in the following models is referred to as a particle, and the subscript "p" is used to refer to properties of the thing being scavenged; however the models apply to any aerosol.

Slinn's inertial model is:

$$E_S = \beta\left(\frac{\rho_p}{1000}\right)^{1/2}\left(\frac{Stk - Stk_*}{Stk - Stk_* + 2/3}\right)^{3/2} \tag{2}$$

where ρ_p is the particle density and Stk is the Stokes number:

$$Stk = \frac{(\rho_p - \rho_a)d^2UC}{9D\mu_a} \tag{3}$$

where ρ_a is the air density, d is the particle diameter, U is the drop velocity, D is the drop diameter, μ_a is the air dynamic viscosity, and C is the Cunningham correction factor:

$$C = 1 + \frac{2\lambda}{d}\left[1.257 + 0.4\exp\left(\frac{-0.55d}{\lambda}\right)\right] \tag{4}$$

λ is the mean free path in air and Stk_* is the critical Stokes number:

$$Stk_* = 1.2 + \frac{1}{12}\left(\frac{\ln(1+Re_D)}{1+\ln(1+Re_D)}\right) \tag{5}$$

where Re_D is the drop Reynolds number:

$$Re_D = \frac{\rho_a DU}{\mu_a} \tag{6}$$

The critical Stokes number Stk_* is the value of Stk below which the particle does not possess sufficient inertia to overcome viscosity and will not come into contact with the drop surface (Beard & Grover, 1974; Friedlander, 1977; Fonda & Herne, 1957; Langmuir, 1948); β is a step function which limits E_S to only the inertial regime: $\beta = 1$ if $Stk > Stk_*$ and $\beta = 0$ otherwise. Using a potential flow solution for flow over a drop gives $Stk_* = \frac{1}{12}$ (Beard & Grover, 1974; Friedlander, 1977; Fonda & Herne, 1957), and Stk_* is slightly greater than unity when using a Stokes flow solution (Beard & Grover, 1974; Fonda & Herne, 1957; Langmuir, 1948). Equation (5) is obtained via an interpolation scheme between these two solutions (Slinn, 1984; Slinn et al., 1977).

As Eq. (2) is an empirical fit to Beard's numerical simulations, it follows that it is subject to the same assumptions as Beard's simulation (Beard & Grover, 1974). Briefly, this simulation traced the path of particles introduced far upstream of a spherical drop, and considered no forces other than those due to the flow and to inertia. These assumptions preclude particle impacts on the drop surface due to the hydrodynamic barrier effect. Accordingly it was assumed that once any particle came within several microns of the drop, other forces, such as an electrostatic force, would become dominant and allow for the particle to penetrate this barrier. Of note, this simulation is identical to the simulation of Langmuir (1948), however due to advances in computing technology it was solved with greater precision. Also, this simulation implicitly assumed that there was no particle bounce off, so that all particles which contact the drop are removed from the system.

The second inertial model is that due to Calvert:

$$E_C = \left(\frac{Stk}{Stk + 0.35}\right)^2 \tag{7}$$

Calvert's model is an empirical fit to the experimental data of Walton and Woolcock (1960) which was obtained from pendant drops and therefore may not be a perfect representation of falling drops, making the application of Calvert's model to falling drops problematic. For example, pendant drops do not experience the same drop oscillations as falling drops, and the wake structure behind a pendant drop will differ from that of a falling drop. Furthermore, the data of Walton and Woolcock (1960) only spanned $0.05 \le Stk \le 1.32$; therefore applying the Calvert model outside of this range may cause problems as well. We note in passing that Calvert's model does not include the critical Stokes number, and the author makes no statement that the model should not be used below this value (Calvert, 1970; Calvert & Englund, 1984). This uncertainty of application is of no bearing here, however, since this paper is only concerned with the inertial range.

3. Experimental comparisons

Numerous experimental studies of particle scavenging by drops exist, however many of these studies do not provide data for $Stk > Stk_*$ (Ardon-Dryer et al., 2015; Beard, 1974; Byrne & Jennings, 1993; Hampl & Kerker, 1972; Hampl, Kerker, Cooke, & Matijevic, 1971; Ladino et al., 2011; Lai, Dayan, & Kerker, 1978; Vohl, Mitra, Kiehl, & Huber, 2001; Wang & Pruppacher, 1977a) and therefore will not be included in the present analysis of inertial regime scavenging. The inertial regime experimental studies considered here are the work of Quérel, Monier, Flossmann, Lemaitre, and Porcheron (2014), Chate and Kamra (1997), Pranesha and Kamra (1996), Leong, Beard, and Ochs (1982), Starr and Mason (1966), and Gunn and Hitschfeld (1950), who performed experiments in the inertial regime using fall towers. Walton and Woolcock (1960) performed experiments in the inertial regime in a vertical wind tunnel. Other inertial regime studies include Ranz and Wong (1956), Hähner, Frank, Dau, Günter, and Ebert (1994), and Waldenmaier (1999) who performed experiments in the inertial regime using horizontal wind tunnels. These studies, however, presented scavenging results only in terms of Stk and D, and due to the flow geometry it could not be assumed that the experiments took place at terminal velocity. This made it impossible to compute groups such as Re_D, which were needed to compare their results to the model predictions, and so they are not considered further hereinafter.

To compare the measured scavenging coefficients, E_m, obtained from the studies cited above, to the predicted values, E_C and E_S, the values of Stk and Re_D were computed from the data provided for each reported data point in the experimental studies cited above. These values were then inserted into Eqs. (2) and (7) to provide E_S and E_C, respectively. Any data that fell outside of the inertial regime were ignored. All reported data were assumed to have been obtained at standard temperature and pressure. For the fall tower studies, the relative velocity between the drop and particles was assumed to be terminal, with the terminal velocity computed using the equation developed by Beard (1976).

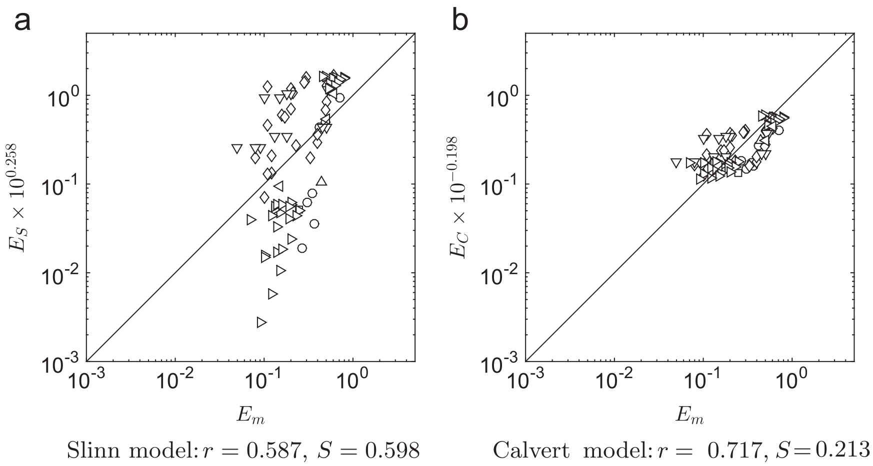

Fig. 1. Predicted versus measured scavenging coefficients comparing (a) Slinn's model and (b) Calvert's model. The data sets are: ○, Walton and Woolcock (1960); □, Quérel et al. (2014); ◇, Chate and Kamra (1997); ▽, Pranesha and Kamra (1996); △, Leong et al. (1982) and Starr and Mason (1966); and ◁, Gunn and Hitschfeld (1950). The Calvert model has better agreement with the surveyed scavenging measurements by virtue of the larger value of r and the smaller value of S for that model. Only experimental data falling within the inertial regime were used.

The model predictions E_S and E_C are plotted against E_m in Fig. 1 along with a unity slope line. Two figures of merit are used to evaluate the similarity of the model to the data. The first is the correlation coefficient:

$$r = \frac{\sum (x_i - \overline{x})(y_i - \overline{y})}{\sqrt{\sum (x_i - \overline{x})^2}\sqrt{\sum (y_i - \overline{y})^2}} \tag{8}$$

The second figure of merit is the standard error of fit of the data to a unity slope line:

$$S = \sqrt{\frac{\sum (y_i - F(x_i))^2)}{n-2}} \tag{9}$$

In the above equations x_i are the experimental measurements, y_i are the model predictions, and F is the unity slope line. Values for r and S are presented in Fig. 1. To provide a more meaningful comparison of the predictive capability of the two models presented in Fig. 1, E_S and E_C were multiplied by a constant that minimized the vertical deviation of the data from the unity slope line. This constant was obtained from the vertical intercept of a least-squares regression on the data in log space. This procedure ensured that the magnitude of r and S was determined by failures of the functional form of E_S and E_C, and not by the lack of a simple multiplicative constant. This constant is included in the label of the ordinate in Fig. 1.

As Fig. 1 shows, the Calvert model does a better job of predicting the data as measured by both r and S. It is noted that the Calvert model is empirically based upon a subset of the data used here, namely the Walton and Woolcock data set. Hence, it is possible that the better performance of the Calvert model is due to the presence of data used in developing that model. To determine if this was the case, the Walton and Woolcock data was removed and new values of r and S were calculated for both models, giving $r=0.624$ and $S=0.588$ for E_S and $r=0.747$ and $S=0.207$ for E_C, showing that the Calvert model continued to perform better, even without the presence of the Walton and Woolcock data. Hence, the Calvert model is the preferred model for predicting scavenging. This result satisfies the first goal of this work, which was to determine which of the two models investigated is preferred for predicting scavenging in the inertial regime.

4. Analysis

In order to improve the models of Slinn and Calvert, the log space residual error, e was computed for each model, where e is defined as:

$$e = \log_{10}(E_m) - \log_{10}(E) \tag{10}$$

Note that the prefactor from Fig. 1 is not used in this equation nor in subsequent equations for e. This residual was related to each of six dimensionless groups ϕ, five of which were identified via a Buckingham Pi analysis, as described below. Specifically, e was related to the dimensionless groups ϕ via a the power law:

$$e = f_1(\phi) = A\phi^b + B \tag{11}$$

where (A, b, B) were found via nonlinear least squares regression. The goodness of the fit was quantified via r and S. This was done for each of the six ϕ considered and the ϕ with the largest r and smallest S were deemed to contribute the most to the residual error and were then used to create an improved model E':

$$E' = E \times 10^{f_1(\phi)} \tag{12}$$

The above process was then repeated, generating a new residual $f_2(\phi)$ for the revised model and correcting it to form a twice-improved model, E''. This process was continued until the most correlated ϕ yielded a correlation coefficient that was less than 0.60. Such a cutoff was needed to give a definite end to the above procedure. The value of 0.6 was somewhat arbitrary; cutoff values smaller than 0.60 resulted in models that were excessively complex and did not visually improve the collapse of the data to the unity slope line in plots such as that presented in Fig. 1.

As noted above, five of the ϕ were obtained using a Buckingham Pi analysis. Assuming that E is a function of D, d, ρ_p, ρ_a, μ_a, U, gravitational acceleration, g, and the particle diffusivity, $\mathcal{D}$, then E will be a function of the five dimensionless groups:

Table 1
Correlations of various dimensionless groups for the residual of E_S.

ϕ	r	S	$f_1(\phi)$
Stk_r	0.854	0.312	$-3.07Stk_r^{0.173}+2.72$
Stk	0.784	0.374	$0.0694Stk^{-2.38}-0.231$
Pe	0.740	0.405	$-1.98\times10^{-12}Pe^{1.18}+0.714$
Re_d	0.701	0.429	$-0.747Re_d^{0.64}+1.4$
Re_D	0.647	0.458	$-1.19\times10^{-6}Re_D^{1.72}+0.613$
Fr	0.114	0.598	$3.19\times10^{13}Fr^{-6.64}+0.25$

Table 2
Correlations of various dimensionless groups for the residual of E_C.

ϕ	r	S	$f_1(\phi)$
Re_D	0.633	0.166	$-4.15\times10^{-16}Re_D^{4.35}-0.101$
Pe	0.463	0.190	$-3.7\times10^{-16}Pe^{1.49}-0.107$
Fr	0.326	0.203	$3.19\times10^{-3}Fr^{0.517}-0.35$
Re_d	0.187	0.211	$-0.065Re_d^{0.683}-0.095$
Stk	0.084	0.214	$5.14\times10^{-3}Stk^{1.69}-0.207$
Stk_r	0.063	0.214	$-9.94\times10^{-5}Stk_r^{-0.885}-0.196$

Re_d, Re_D, Stk, the Péclet number, Pe, and the Froude number, Fr. Additionally a relative Stokes number, Stk_r was developed for this analysis:

$$Stk_r=\log_{10}\left(\frac{Stk}{Stk_*}\right) \tag{13}$$

which cannot be obtained from the Buckingham Pi analysis. This dimensionless group is a measure of the particle's inertia relative to the critical value, and is a measure of how far into the inertial regime an experimental condition lies. It was thought to provide a measure of inertia potentially better than Stk alone, a supposition borne out by the following results.

The resulting functions for the first iteration of the above process, f_1, are presented in Tables 1 and 2 for the Slinn and Calvert models, respectively. Note that the subscripts S and C will be used for Slinn and Calvert, respectively. These tables show that the two model residuals are best described by different dimensionless groups: e_S is best described by Stk_r and e_C is best described by Re_D.

Tables 3 and 4 present the residual, e', between E_m and E':

$$e'=\log_{10}(E_m)-\log_{10}(E') \tag{14}$$

as well as the power law relationships, $f_2(\phi)$, relating ϕ and e'. As Table 4 shows, the modified Calvert model is not well correlated with any of the investigated dimensionless groups, its correlation coefficient being less than 0.60 for all ϕ considered. Thus, the modified Calvert model is E'_C:

$$E'_C=E_C\times10^{-4.15\times10^{-16}Re_D^{4.35}}\times10^{-0.101} \tag{15}$$

Table 3 shows a significant correlation between e'_S and Re_D, and so the above process was repeated yet again for that model, resulting in the correlations shown in Table 5. As all of the correlation coefficients are less than 0.60 in Table 5, we consider the doubly modified model as the revised Slinn model:

$$E''_S=E'_S\times10^{f_2(Re_D)} \tag{16}$$

or, via substitution:

$$E''_S=E_S\times10^{-3.07Stk_r^{0.173}}\times10^{-2.61\times10^{-14}Re_D^{3.9}}\times10^{2.905} \tag{17}$$

Equations (17) and (15) are the improved versions of the Slinn and Calvert models, respectively, which achieve the second goal of this work, to improve upon the accuracy of their original versions. These equations are reproduced below:

$$E^*_S=E''_S=E_S\times10^{-3.07Stk_r^{0.173}}\times10^{-2.61\times10^{-14}Re_D^{3.9}}\times10^{2.905} \tag{18}$$

$$E^*_C=E'_C=E_C\times10^{-4.15\times10^{-16}Re_D^{4.35}}\times10^{-0.101} \tag{19}$$

Plots of the original and improved Slinn and Calvert models are presented in Fig. 2, showing significantly improved collapse of the data to the unity slope line for the improved models.

Table 3
Correlations of various dimensionless groups for the residual of E'_S.

ϕ	r	S	$f_2(\phi)$
Re_D	0.803	0.186	$-2.61\times10^{-14}Re_D^{3.9}+0.185$
Pe	0.568	0.257	$-6.68\times10^{-16}Pe^{1.49}+0.162$
Stk_r	0.272	0.301	$-6.06\times10^{-15}Stk_r^{-4.11}+0.009$
Stk	0.261	0.302	$7.24\times10^{-6}Stk^{-8.15}-0.036$
Fr	0.192	0.307	$9.89\times10^{-8}Fr^{1.55}-0.020$
Re_d	0.158	0.308	$-0.098Re_d^{0.59}+0.144$

Table 4
Correlations of various dimensionless groups for the residual of E_C'.

ϕ	r	S	$f_2(\phi)$
Fr	0.432	0.15	$0.584Fr^{0.0913}-1.140$
Re_D	0.263	0.160	$0.395Re_D^{0.052}-0.549$
Stk_r	0.228	0.162	$-0.063Stk_r^{-0.217}+0.091$
Pe	0.167	0.164	$0.060Pe^{0.069}-0.263$
Stk	0.141	0.165	$-4.69\times10^{-24}Stk^{-38.3}$
Re_d	0.130	0.165	$-0.169Re_d^{-0.202}+0.153$

Table 5
Correlations of various dimensionless groups for the residual of E_S''.

ϕ	r	S	$f_3(\phi)$
Stk_r	0.567	0.153	$-8.04\times10^{-15}Stk_r^{-4.11}+0.011$
Re_d	0.390	0.171	$-0.222Re_d^{-0.504}+0.179$
Fr	0.348	0.174	$-3.78Fr^{-0.384}+0.232$
Re_D	0.326	0.176	$-0.731Re_D^{-0.451}+0.057$
Pe	0.322	0.176	$-276Pe^{-0.399}+0.070$
Stk	0.200	0.182	$0.032Stk^{0.978}-0.034$

5. Discussion

We now address the question of whether the dimensionless groups used in revising the equations of Slinn and Calvert may provide insight on additional mechanisms governing scavenging in the inertial regime. The dimensionless groups Stk_r and Re_D were used to revise the models. Stk_r is discussed first.

Figure 3 presents the residual, e_S, versus Stk_r, showing that e_S is high when Stk_r is near zero, but decreases as Stk_r increases. This implies that E_S under-predicts scavenging near the transition to the inertial regime, but improves as Stk_r increases. This indicates that there exists some mechanism that is not well accounted for in E_S which plays a role in scavenging during the transition to inertially dominated scavenging. In comparison, Stk_r is the least well correlated dimensionless group for e_C.

Recall that E_S is solely based upon inertial impaction simulations by Slinn et al. (1977) and Beard and Grover (1974), while E_C is solely based upon experimental measurements of particle collection by pendant drops performed by Calvert (1970) and Walton and Woolcock (1960). This provides information regarding what additional mechanisms could be contributing to scavenging in the transition to the inertial regime. The fact that e_C is uncorrelated to Stk_r for even freely falling drops indicates that this mechanism is likely present for both pendant drops and for drops in free fall. This rules out any mechanisms which rely on the back half of the drop, as that is where a pendant drop would be supported. It also likely rules out any mechanism related to drop oscillations as a pendant drop will be relatively pinned due to its support.

A possible mechanism fitting these requirements would be the inertial compression of the particle phase on the front hemisphere of the drop. This mechanism is an inertial enhancement of diffusional deposition caused by inertially increasing the particle concentration near the drop surface. It was proposed by de la Mora and Rosner (1982), and would correspond to larger scavenging near $Stk_r=0$. This is because as particles approach the drop they will deviate from their streamlines due to inertia; as Stk_r increases this deviation becomes larger and the resulting scavenging increases. However, at low Stk_r very few particles will be deflected enough to allow for inertial impaction on the drop. Instead the majority of affected particles will become more closely packed near the drop surface, resulting in an increase in the local concentration of particles near the drop surface relative to the freestream concentration. Because of the particle phase compression there is an increased concentration gradient near the drop, which will result in a greater mass transfer of the particle phase to the drop surface via diffusional deposition.

The contribution of this mechanism to scavenging will diminish, however, as the inertia of the particles is increased. This is due to two mechanisms: first more particles will be scavenged due to inertial impaction as Stk increases; second, as Stk increases the required time for a particle to travel around the drop will become significantly shorter than its relaxation time, meaning that there will be less time for the inertial compression of the particle phase to enhance mass transfer to the drop surface. As this mechanism would be present in any of the experimental measurements considered here, and it agrees with the trend in Fig. 3, it is a possible explanation for some of the residual observed with the Slinn model.

The other dimensionless group that was well correlated with the model residuals was Re_D, as shown in Tables 2 and 3. Figure 4 presents plots of the residual versus Re_D for both models, showing similar behavior for both models. Hence, the mechanism which Re_D describes is most likely not accounted for by either model. A possible mechanism that could account for this trend is wake capture of particles. Wake capture occurs when a particle traverses the front end of the drop without

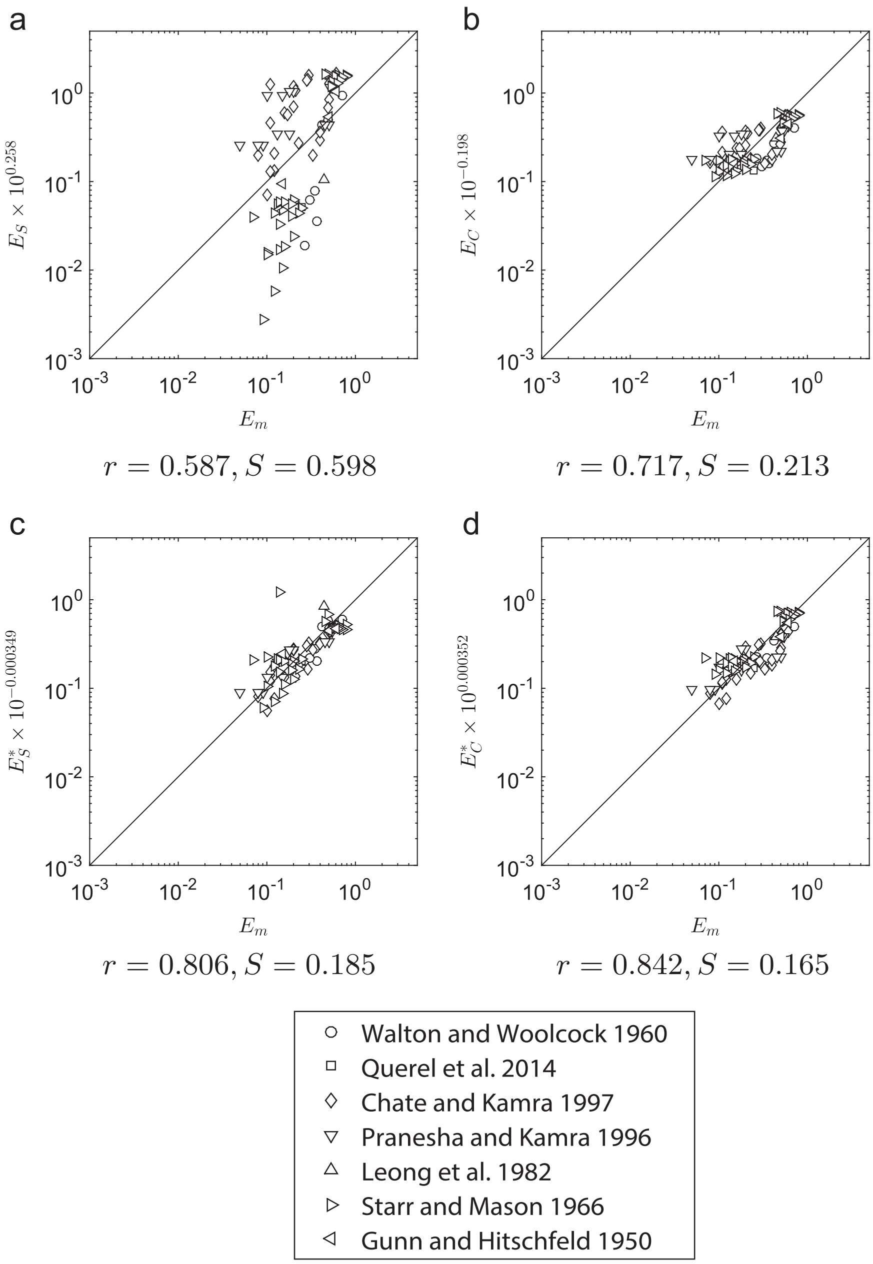

Fig. 2. Plots of model prediction versus experimental data: (a) and (b) are the unmodified Slinn and Calvert models, respectively; (c) and (d) are the final, modified Slinn and Calvert models, respectively.

being scavenged but is then pulled into the recirculating region in the drop wake and is ultimately deposited on the back side of the drop after one or more passes in this recirculating region. Wake capture is often used to explain scatter in experimental data (Beard, 1974; Goldshmid & Calvert, 1963; Quérel et al., 2014; Wang & Pruppacher, 1977b). However, to the authors' knowledge there has been no rigorous study of the wake capture of particles by a falling drop. Sakamoto and Haniu (1990) showed that the wake dynamics for a sphere are primarily a function of Re_D, with vortex shedding beginning to occur at $Re_D \sim 300$. This corresponds with the trends in Fig. 4, as there is a large drop off in the residual for $Re_D > 600$, which is in the vortex shedding regime. If wake capture is playing a significant role in particle scavenging it would follow that once the wake becomes unstable during vortex shedding the likelihood of particle capture by this method is reduced significantly, and would lead to the observed decrease in the residual. Furthermore, wake capture of particles is not included in Beard's simulations, and is unlikely to have an effect in Walton and Woolcock's data due to their experimental apparatus, which used a vertical wind tunnel, and, instead of a freely floating drop, a pendent drop. This drop was supported with a fixed structure which would make the wake different from that of a freely falling drop. Because the observed trend approximately

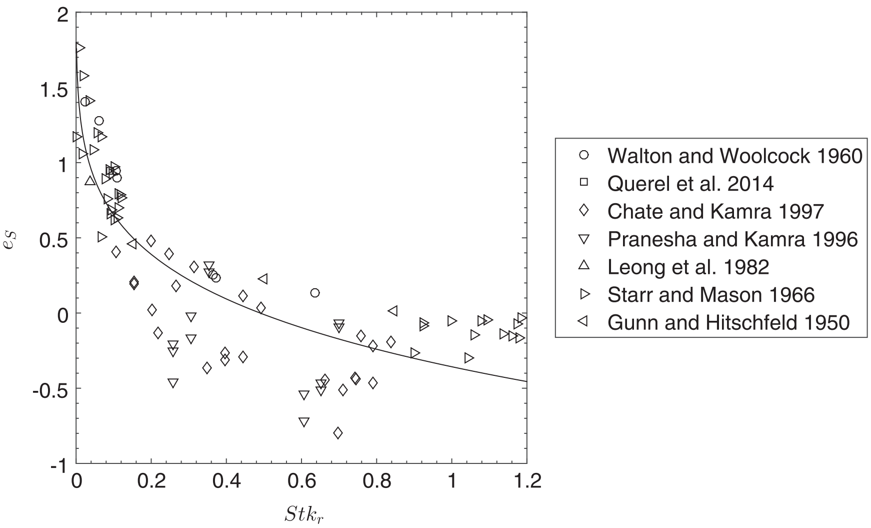

Fig. 3. Relationship between the residual, e_S, and Stk_r for the unmodified Slinn model, E_S.

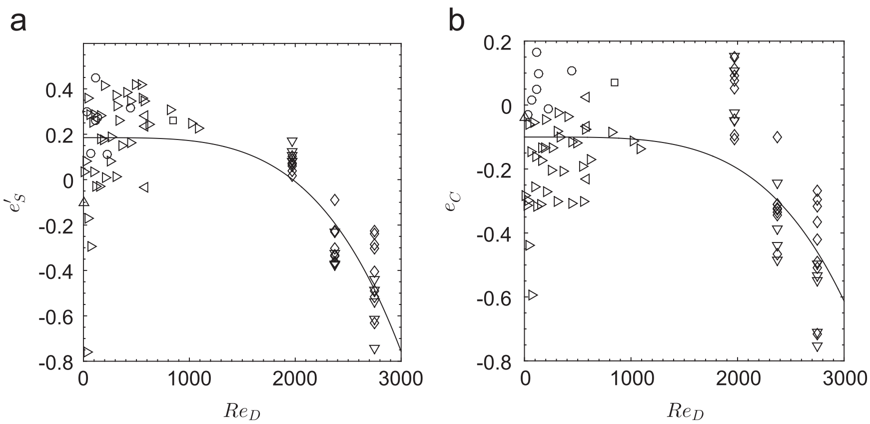

Fig. 4. Plots of residual versus Re_D for: (a) the Slinn model and (b) the Calvert model. The data sets are: ○, Walton and Woolcock (1960); □, Quérel et al. (2014); ◇, Chate and Kamra (1997); ▽, Pranesha and Kamra (1996); △, Leong et al. (1982) and Starr and Mason (1966); and ◁, Gunn and Hitschfeld (1950).

matches the expected trend for the onset of vortex shedding and because it is reasonable to conclude that this mechanism is not accounted for in either model, it is possible that wake capture plays a role in scavenging in the inertial regime.

6. Conclusion

This work shows that the Calvert model better predicts published experimental scavenging data in the inertial regime. Modifications to the two models are given in Eqs. (15) and (17), both of which better describe the measured results than either unmodified model. Two mechanisms other than inertial impaction were identified as playing a measurable role in scavenging within the inertial regime based upon the parametric study of the model residuals conducted. The dimensionless group Stk_r indicates an inertial mechanism at play, likely the compression of the particle phase near the front hemisphere of the drop. The dimensionless group Re_D indicates an advective mechanism at play, perhaps wake dynamics due to the drop off at high Re_D. Further experimental investigation is required to confirm that these are, in fact, the correct mechanisms described by the identified dimensionless groups.

References

Adams, P. J., & Seinfeld, J. H. (2002). Predicting global aerosol size distributions in general circulation models. *Journal of Geophysical Research*, *107* AAC 4-1–AAC 4-23.

Ardon-Dryer, K., Huang, Y. W., & Cziczo, D. J. (2015). Laboratory studies of collection efficiency of sub-micrometer aerosol particles by cloud droplets on a single droplet basis. *Atmospheric Chemistry and Physics Discussions*, *15*, 6207–6236.
Beard, K. V. (1974). Experimental and numerical collision efficiencies for submicron particles scavenged by small raindrops. *Journal of the Atmospheric Sciences*, *31*, 1595–1603.
Beard, K. V. (1976). Terminal velocity and shape of cloud and precipitation drops aloft. *Journal of the Atmospheric Sciences*, *33*, 851–864.
Beard, K. V., & Grover, S. N. (1974). Numerical collision efficiencies for small raindrops colliding with micron size particles. *Journal of the Atmospheric Sciences*, *31*, 543–550.
Byrne, M. A., & Jennings, S. G. (1993). Scavenging of sub-micrometer aerosol particles by water drops. *Atmospheric Environment*, *27A*, 2099–2105.
Calvert, S. (1970). Venturi and other atomizing scrubbers efficiency and pressure drop. *AIChE Journal*, *16*, 392–396.
Calvert, S., & Englund, H. M. (1984). *Handbook of air pollution technology*. New York: Wiley.
Calvert, S., & Goldshmid, J. (1972). *Wet scrubber system study*: *Scrubber handbook*. Technical report. EPA.
Chate, D. M., & Kamra, A. K. (1997). Collection efficiencies of large water drops collecting aerosol particles of various densities. *Atmospheric Environment*, *31*, 1631–1635.
Chate, D. M., Murugavel, K. A., Tiwari, S., & Beig, G. (2011). Below-cloud rain scavenging of atmospheric aerosols for aerosol deposition models. *Atmospheric Research*, *99*, 528–536.
Davenport, H. M., & Peters, L. K. (1978). Field studies of atmospheric particulate concentration changes during precipitation. *Atmospheric Environment*, *12*, 997–1008.
de la Mora, J. F., & Rosner, D. E. (1982). Effects of inertia on the diffusional deposition of small particles to spheres and cylinders at low Reynolds numbers. *Journal of Fluid Mechanics*, *125*, 379–395.
Fonda, A., & Herne, H. (1957). *Hydrodynamic capture of particles by spheres*. Mines Research Establishment Report 2086.
Friedlander, S. K. (1977). *Friedlander, smoke, dust, and haze*. New York: Oxford University Press.
Goldshmid, Y., & Calvert, S. (1963). Small particle collection by supported liquid drops. *AIChE Journal*, *9*, 352–358.
Greenfield, S. M. (1957). Rain scavenging of radioactive particulate matter from the atmosphere. *Journal of Meteorology*, *14*, 115–125.
Gunn, K., & Hitschfeld, W. (1950). A laboratory investigation of the coalescence between large and small water-drops. *Journal of Meteorology*, *8*, 7–16.
Hähner, Frank, Dau, Günter, & Ebert, Fritz. (1994). Inertial impaction of aerosol particles on single and multiple spherical targets. *Chemical Engineering & Technology*, *17*, 88–94.
Hampl, V., & Kerker, M. (1972). Scavenging of aerosol particles by a falling water droplet. Effect of particle size. *Journal of Colloid and Interface Science*, *40*, 305–308.
Hampl, V., Kerker, M., Cooke, D. D., & Matijevic, E. (1971). Scavenging of aerosol particles by a falling water droplet. *Journal of the Atmospheric Sciences*, *28*, 1211–1221.
Hinds, W. C. (1982). *Aerosol technology: Properties, behavior, and measurement of airborne particles*. NY, New York: Wiley-Interscience.
Kissell, F. N. (2003). *Handbook of dust control in mining*. NIOSH Publication Number 2003-147. Cincinnati, OH: NIOSH Publications.
Ladino, L., Stetzer, O., Hattendorf, B., Günther, D., Croft, B., & Lohmann, U. (2011). Experimental study of collection efficiencies between submicron aerosols and cloud droplets. *Journal of the Atmospheric Sciences*, *68*, 1853–1864.
Lai, K. Y., Dayan, N., & Kerker, M. (1978). Scavenging of aerosol particles by a falling water droplet. *Journal of the Atmospheric Sciences*, *35*, 674–682.
Langmuir, I. (1948). The production of rain by a chain reaction in cumulus clouds at temperatures above freezing. *Journal of Meteorology*, *5*, 175–192.
Leong, K. H., Beard, K. V., & Ochs, H. T., III (1982). Laboratory measurements of particle capture by evaporating cloud drops. *Journal of the Atmospheric Sciences*, *39*, 1130–1140.
Levich, V. G. (1962). *Physicochemical hydrodynamics*. New Jersey: Prentice-Hall.
Park, S. H., Jung, C. H., Jung, K. R., Lee, B. K., & Wet, L. K. W. (2005). scrubbing of polydisperse aerosols by freely falling droplets. *Journal of the Atmospheric Sciences*, *36*, 1444–1458.
Pranesha, T. S., & Kamra, A. K. (1996). Scavenging of aerosol particles by large water drops 1. Neutral case. *Journal of Geophysical Research*, *101*, 23,373–23,380.
Quérel, A., Monier, M., Flossmann, A. I., Lemaitre, P., & Porcheron, E. (2014). The importance of new collection efficiency values including the effect of rear capture for the below-cloud scavenging of aerosol particles. *Atmospheric Research*, *142*, 57–66.
Ranz, W. E., & Wong, J. B. (1956). Impaction of dust and smoke particles. *Industrial & Engineering Chemistry*, *44*, 1371–1381.
Roeckner, E., Bäuml, G., Bonaventura, L., Brokopf, R., Esch, M., Giorgetta, M., et al. (2003). *The atmospheric general circulation model ECHAM 5. Part i: Model description*. Technical report. MPI für Meteorologie.
Sakamoto, H., & Haniu, H. (1990). A study on vortex shedding from spheres in a uniform flow. *Journal of Fluids Engineering*, *112*, 386–392.
Schnelle, K. B., & Brown, C. A. (2002). Air pollution control technology handbook. In *The mechanical engineering handbook series*. Boca Raton, FL: CRC Press.
Seinfeld, J. H., & Pandis, S. N. (2006). *Atmospheric chemistry and physics: From air pollution to climate change*. New Jersey: Wiley & Sons.
Slinn, W. G. N. (1977). Precipitation scavenging: Some problems, approximate solutions, and suggestions for future research. In R. G. Semonin, & R. W. Beadle (Eds.), *Precipitation scavenging* (*1974*): *Proceedings of a symposium held at Champaign*, *Illinois*, *October 14–18*, *1974. ERDA symposium series*, Springield, VA (Vol. 41, pp. 1–60).
Slinn, W. G. N. (1984). Precipitation scavenging. *Atmospheric Science and Power Production*, 466–532.
Starr, J. R., & Mason, B. J. (1966). The capture of airborne particles by water drops and simulated snow crystals. *Quarterly Journal of the Royal Meteorological Society*, *92*, 490–499.
Vohl, O., Mitra, S. K., Kiehl, K., & Huber, G. (2001). A wind tunnel study of turbulence effects on the scavenging of aerosol particles by water drops. *Journal of the Atmospheric Sciences*, *58*, 3064–3072.
Waldenmaier, M. (1999). Measurements of inertial deposition of aerosol particles in regular arrays of spheres. *Journal of Aerosol Science*, *30*, 1281–1290.
Walton, W. H., & Woolcock, A. (1960). The suppression of airborne dust by water spray. *International Journal of Air Pollution*, *3*, 129–153.
Wang, H. C., Leong, K. H., Stukel, J. J., & Hopke, P. K. (1983). The effects of thermophoresis and diffusiophoresis on the collection of charged sub-μm particles by charged droplets. *Atmospheric Environment*, *17*, 2533–2537.
Wang, P. K., & Pruppacher, H. R. (1977a). Acceleration to terminal velocity of cloud and raindrops. *Journal of Applied Meteorology*, *16*, 276–280.
Wang, P. K., & Pruppacher, H. R. (1977b). An experimental determination of the efficiency with which aerosol particles are collected by water drops in subsaturated air. *Journal of the Atmospheric Sciences*, *34*, 1664–1669.
Wang, X., Zhang, L., & Moran, M. D. (2010). Uncertainty assessment of current size-resolved parameterizations for below-cloud particle scavenging by rain. *Atmospheric Chemistry and Physics*, *10*, 5685–5705.
Webster, H. N., & Thomson, D. J. (2014). *The NAME wet deposition scheme*. Technical report. Forecasting research technical report.